# Novel approach to joint 3D inversion of EM and potential field data using Gramian constraints

**Michael S. Zhdanov[1,2], Yue Zhu[2], Masashi Endo[1] and Yuri Kinakin[3] demonstrate how joint inversion using Gramian constraints may enhance subsurface imaging of the mineral targets.**

One of the major challenges in interpretation of geophysical data remains the ability to jointly invert multiple geophysical datasets for self-consistent 3D earth models of different physical properties. To date, various attempts at 3D joint inversion have been based on either correlations between different physical properties, or by introducing structural similarities. In addition, there could be both physical property and structural correlations between the different earth models, and these complexities cannot be captured by any existing joint inversion techniques. Note that, in practical applications, empirical or statistical correlations between different physical properties may exist, but their specific form may be unknown. In this situation, one can use a method of joint inversion, which does not require a priori knowledge about specific empirical or statistical relationships between the different model parameters and/or their attributes. This approach to the joint inversion of multimodal geophysical data uses Gramian spaces of model parameters and Gramian constraints, computed as determinants of the corresponding Gram matrices of the multi-modal model parameters and/or their attributes. This method, recently introduced by Zhdanov et al. (2012), has been shown to be a generalized method of joint inverting any number and combination of geophysical datasets, and includes extant methods based on correlations and/or structural constraints of the multiple physical properties as special case. The method is illustrated by two case studies. We present the results of joint inversion of airborne gravity gradiometer (AGG) and magnetic data collected by Fugro Airborne Surveys in the area of McFaulds Lake located in northwestern Ontario. We also jointly invert airborne magnetic and electromagnetic data from the Lac de Gras region of the Northwest Territories of Canada. These case studies demonstrate how joint inversion using Gramian constraints may enhance subsurface imaging of the mineral targets.

One of the most challenging problems of the inversion of electromagnetic and potential field data is their nonuniqueness. Joint inversion is a technique capable of solving this problem by recovering more than one physical property jointly from a multimodal geophysical data. It is often the case in mature mining districts that there are several independent datasets available within the survey area, which makes the joint inversion more feasible and cost effective. Different geophysical datasets are sensitive to different physical properties. The first challenge in any joint inversion is that one has to make an assumption about the relationship between the different properties. The direct joint parameter inversion method assumes a direct functional relationship between the different parameters (Heincke et al., 2006; Jegen et al., 2009). The cross gradient constraint enforces the structural similarities between the different properties (Gallardo et al., 2003; Zhdanov et al., 2012; Zhdanov 2015) introduced the Gramian constraint, which can be treated as a generalized correlation between the different parameters. By specifying a type of Gramian constraint, one can enforce polynomial, gradient, or any other complex correlations.

We illustrate the novel method of joint inversion using the Gramian constraints by two case studies: 1) joint inversion of airborne gravity gradiometer (AGG) and magnetic data collected by Fugro Airborne Surveys in the area of the McFaulds Lake located in northwestern Ontario; and 2) joint inversion of airborne magnetic (total magnetic intensity – TMI) and electromagnetic (EM) data from the Lac de Gras region of the Northwest Territories of Canada, where the target kimberlites are characterized by a strong remnant of magnetization and anomalous conductivity.

## Principles of joint inversion using Gramian constraints

Let us consider forward geophysical problems for multiple geophysical data sets. These problems can be described by the following operator relationships:

$$d^{(i)} = A^{(i)}\left(m^{(i)}\right), i = 1, 2, 3, \cdots, n;$$

where, in a general case, $A^{(i)}$ is a nonlinear operator, $d^{(i)}$ $(i = 1, 2, 3, \cdots, n)$ are different observed data sets (which may have different physical natures and/or parameters), and $m^{(i)}$ $(i = 1, 2, 3, \cdots, n)$ are the unknown sets of model parameters.

[1] *TechnoImaging.*
[2] *The University of Utah.*
[3] *Rio Tinto, Diavik Diamond Mines.*
[*] *Corresponding author, E-mail: mzhdanov@technoimaging.com*

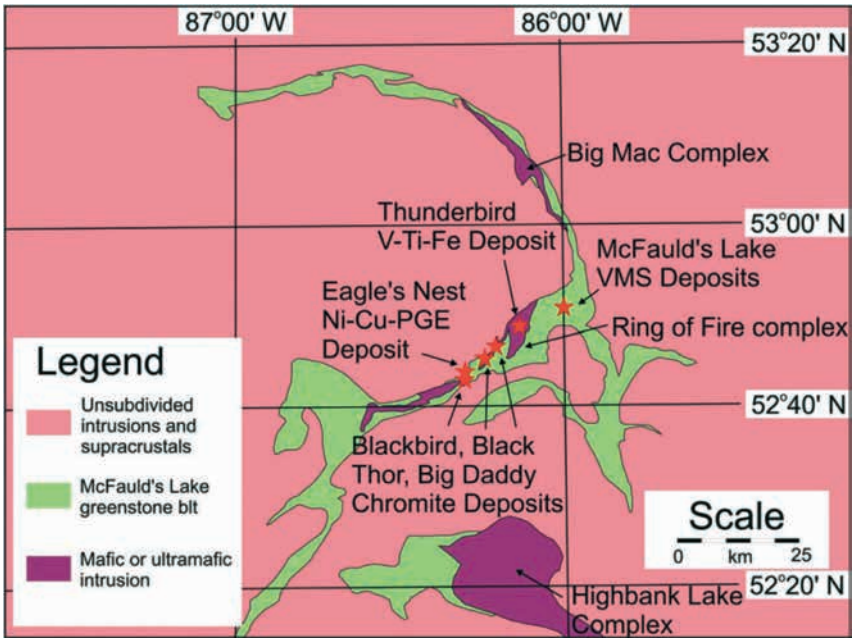


*Figure 1* Geological sketch map with known mineralization in the Ring of Fire region (from Mungall et al., 2010).

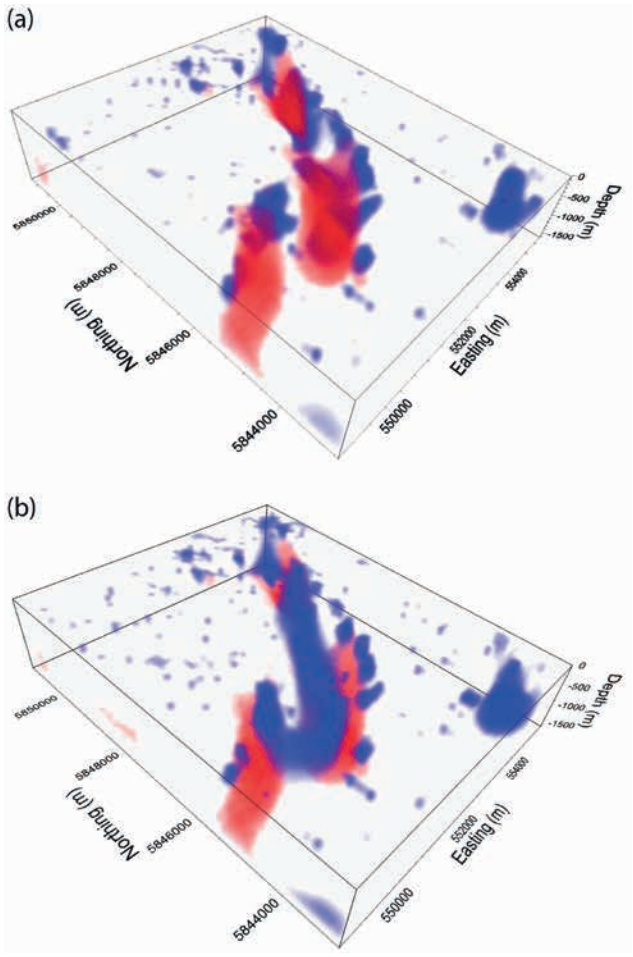


*Figure 2* 3D views of density (blue; > 2.87 g/cm3) and magnetic susceptibility (red; 0.006 SI) recovered from (a) joint inversion using Gramian constraints, (b) independent inversions.

Note that, in a general case, different model parameters may have different physical dimensions (e.g., density is measured in g/cm$^3$, resistivity is measured in Ohm-m, etc.). It is convenient to introduce the dimensionless weighted model parameters, $\tilde{m}^{(i)}$, defined as follow: $\tilde{m}^{(i)} = W_m^{(i)} m^{(i)}$,

where $W_m^{(i)}$ is the corresponding linear operator of model weighting (Zhdanov, 2002).

The Gramian of a system of model parameters $\tilde{m}^{(1)}, \tilde{m}^{(2)}, \ldots, \tilde{m}^{(n-1)}, \tilde{m}^{(n)}$ is introduced as a determinant, $G\left(\tilde{m}^{(1)}, \tilde{m}^{(2)}, \cdots, \tilde{m}^{(n-1)}, \tilde{m}^{(n)}\right)$, of the Gramian matrix of a set of functions, $\tilde{m}^{(1)}, \tilde{m}^{(2)}, \ldots, \tilde{m}^{(n-1)}, \tilde{m}^{(n)}$ (Zhdanov et al., 2012; Zhdanov, 2015). This provides a measure of correlation between the different model parameters or their attributes. By imposing the additional requirement minimizing the Gramian in regularized inversion, we obtain multi-modal inverse solutions with enhanced correlations between the different model parameters or their attributes. For example, in the case of two model parameters (e.g., density and magnetic susceptibility), the Gramian is computed as follows:

$$G\left(\tilde{m}^{(1)}, \tilde{m}^{(2)}\right) = \begin{vmatrix} \left(\tilde{m}^{(1)}, \tilde{m}^{(1)}\right) & \left(\tilde{m}^{(1)}, \tilde{m}^{(2)}\right) \\ \left(\tilde{m}^{(2)}, \tilde{m}^{(1)}\right) & \left(\tilde{m}^{(2)}, \tilde{m}^{(2)}\right) \end{vmatrix} = \left\|\tilde{m}^{(1)}\right\|^2 \left\|\tilde{m}^{(2)}\right\|^2 \left[1 - \eta^2\left(\tilde{m}^{(1)}, \tilde{m}^{(2)}\right)\right],$$

with $(\cdot,\cdot)$ standing for the inner product in the corresponding Gramian space (Zhdanov, 2015). The coefficient, $\eta$, can be treated as a correlation coefficient between two parameters, $\tilde{m}^{(1)}$ and $\tilde{m}^{(2)}$:

$$\eta\left(\tilde{m}^{(1)}, \tilde{m}^{(2)}\right) = \frac{\left(\tilde{m}^{(1)}, \tilde{m}^{(2)}\right)}{\left\|\tilde{m}^{(1)}\right\| \ \left\|\tilde{m}^{(2)}\right\|}.$$

The last expressions show that the Gramian provides a measure of correlation between two parameters, $m^{(1)}$ and $m^{(2)}$. Indeed, the Gramian goes to zero, when the correla-

tion coefficient is close to one, which corresponds to linear correlation. This property shows that by minimizing a parametric functional with the Gramian constraint, we enforce some linear correlation between the model parameters.

For a regularized solution of the inverse problem, we introduce a parametric functional with Gramian stabilizers,

$$P^{\alpha}\left(\tilde{m}^{(1)},\tilde{m}^{(2)},\cdots,\tilde{m}^{(n)}\right) = \sum_{i=1}^{n}\left\|\tilde{A}^{(i)}\left(\tilde{m}^{(i)}\right)-\tilde{d}^{(i)}\right\|_{D}^{2}+\alpha c_1\sum_{i=1}^{n}S_{MN,MS,MGS}^{(i)}+\alpha c_2 G\left(\tilde{m}^{(1)},\cdots,\tilde{m}^{(n)}\right),$$

where $\tilde{A}^{(i)}\left(\tilde{m}^{(i)}\right)$ are the weighted predicted data, $\tilde{A}^{(i)}\left(\tilde{m}^{(i)}\right)=W_d^{(i)}A^{(i)}\left(\tilde{m}^{(i)}\right)$, $\alpha$ is the regularization parameter, and $c_1$ and $c_2$ are the weighting coefficients determining the weights of the different stabilizers in the parametric functional.

The terms $S_{MN}^{(i)}$, $S_{MS}^{(i)}$ and $S_{MGS}^{(i)}$ are the stabilizing functionals, based on minimum norm, minimum support, and minimum gradient support constraints, respectively (Zhdanov, 2009, 2015). The solution of the minimization problem for the parametric functional with the Gramian stabilizers can be achieved by using the re-weighted conjugate gradient method, as discussed in Zhdanov (2015).

## Case study 1: inversion of the airborne geophysical data in McFaulds Lake, Ontario

McFaulds Lake is located in northwestern Ontario. It contains the 'Ring of fire', which is a roughly north-south trending Archean greenstone belt (Figure 1). This westward-concave belt sits on the west edge of the James Bay Lowland in far northwestern Ontario and is currently a focus of major mining explorations. Various economic mineral deposit types are known to exist in this area, including magmatic Ni-Cu-PGE, V-Ti-Fe and chromite mineralization, volcanic massive sulfide (VMS) mineralization and diamonds hosted by kimberlite.

Airborne geophysical surveys were carried out in the MacFaulds Lake region by Fugro between 2010 and 2011, collecting airborne gravity gradiometry (AGG) and magnetic data. This project was collaboratively operated between the Ontario Geological Survey (OGS) and the Geological Survey of Canada (GSC).

In this case study, we focused on a subset of the AGG and magnetic data covering the southern part of greenstone belt. The inversion domain covers the area of 40 x 40 km$^2$ to 2 km depth and 50 m$^3$ cells, resulting in roughly 34 million cells and 1,080,000 data points. We used all six provided AGG components and TMI, and inverted for density and susceptibility. Both physical properties converged well,

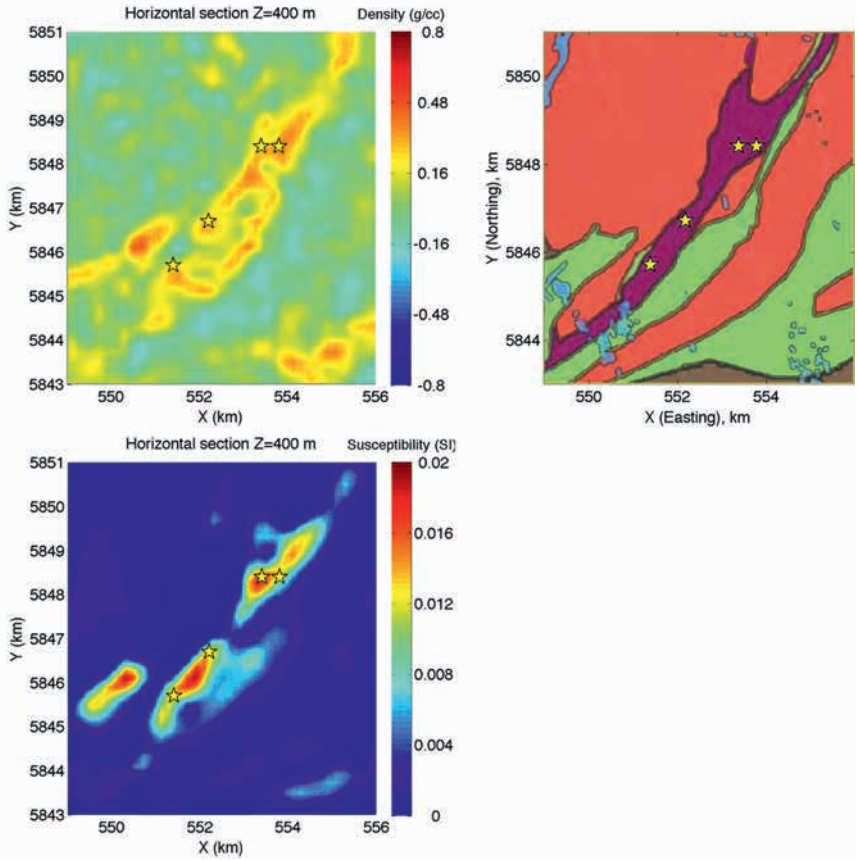


***Figure 3*** *Comparison among the geological sketch map, horizontal anomalous density, and susceptibility slices, recovered from joint inversion. The predicted anomalous density distribution is shown at top left. The predicted susceptibility is shown at bottom left. The stars indicate the locations of four major mineral deposits.*

reaching 6% and 3% L2 norm misfit, respectively, after 100 iterations, which took 16 hours on four cluster nodes using 2 GPUs per node.

Figure 2 shows 3D views of 3D density and magnetic susceptibility distributions recovered from joint inversion using Gramian constraints and from independent inversions. Figure 3 shows a comparison between the geological map and recovered density and magnetic susceptibility distributions from joint inversion using Gramian constraints. One can see that both anomalous density and susceptibility agree well with known mineral deposits, and we believe that recovered 3D physical property models from joint inversion (Figure 2a) is more reliable than the model recovered from independent inversions (Figure 2b).

Figure 4 shows the cross plot of the predicted anomalous density and susceptibility for both the independent and joint inversions. Each point in the cross plot represents a model cell in the inversion (limited to a smaller region around the Big Daddy deposit). This figure gives convincing evidence that the joint inversion indeed recovers some relationship between the density and susceptibility within the mine deposits that we are interested in.

## Case study 2: joint inversion of airborne TMI and frequency domain EM data in the Northwest Territories of Canada

We applied the developed joint inversion algorithm to the field airborne data collected for kimberlite exploration. The survey area belongs to the Slave Structural Province in the Northwest Territories of Canada, which forms a distinct cratonic block within the Canadian Precambrian Shield. The eastern domain of the Slave Geological Province, which underlies the Lac de Gras area, has been more productive for

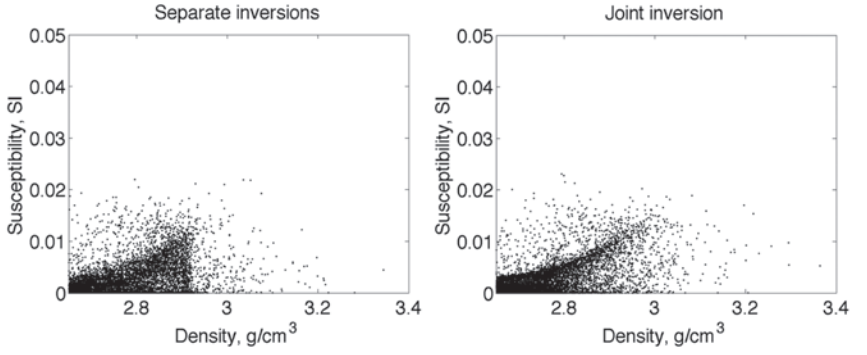


*Figure 4* *Cross plots of the predicted density and susceptibility. The left panel shows the plot for the predicted model computed by the independent inversions, and the right panel is the plot obtained by the joint inversion. The model cells plotted here are centered around the Big Daddy chromite deposit.*

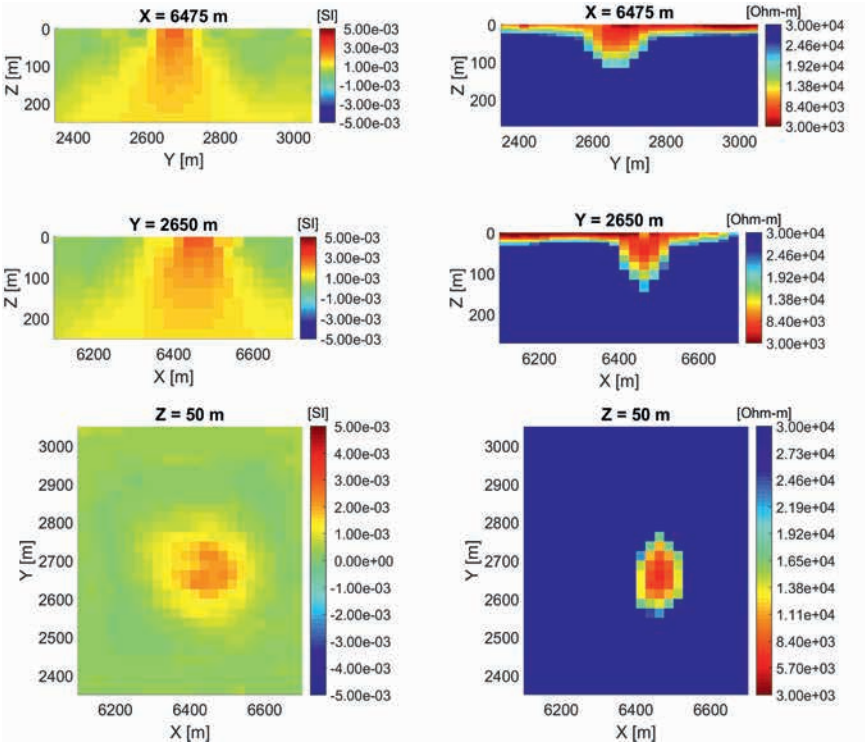


*Figure 5* *Vertical and horizontal sections of the recovered magnetization and resistivity models obtained by independent 3D inversions of the TMI and AEM data. The left panels present the magnitude of magnetization vector, while the right panels show the resistivity model in the survey area.*

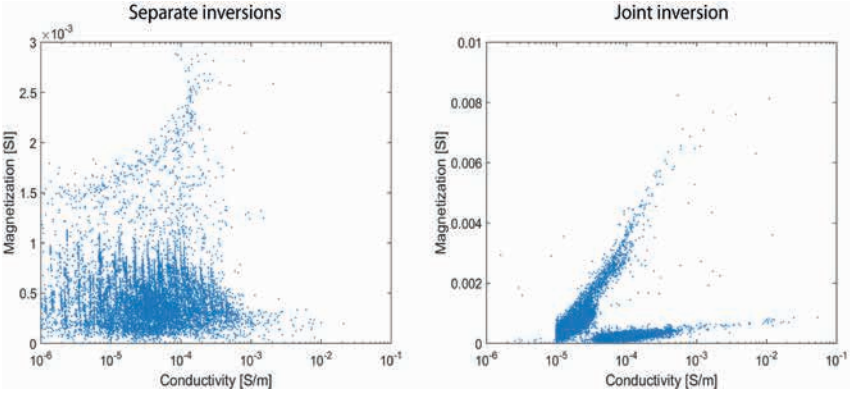


*Figure 6* Cross plots of the predicted magnitude of the magnetization vector versus the anomalous conductivity. Left panel shows the plot for predicted model computed by the independent inversions, and the right panel is the plot obtained by the joint inversion.

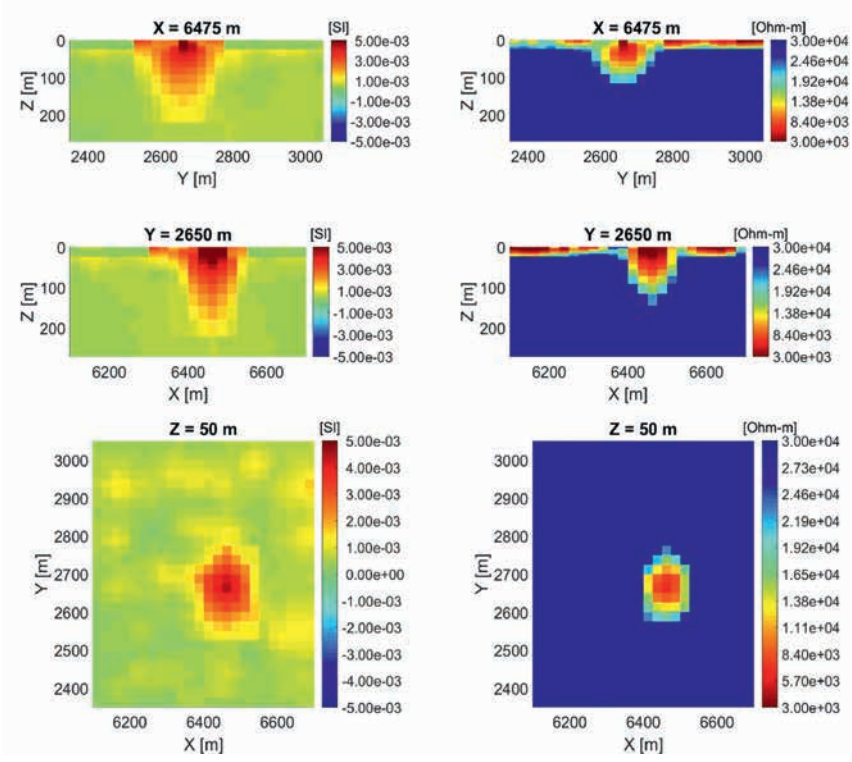


*Figure 7* Vertical and horizontal sections of the recovered magnetization and resistivity models obtained by the joint 3D inversion of the TMI and AEM data. The left panels present the magnitude of the magnetization vector, while the right panels show the resistivity model in the survey area.

kimberlite exploration than the western domain. We applied the joint inversion to total magnetic intensity (TMI) and frequency domain electromagnetic (EM) data collected over an area with the known kimberlite pipe. In the first step of the analysis, independent inversions of the TMI and EM data sets were conducted. Using the 1D AEM inversion result as the starting model and setting the half-space background conductivity to $10^{-5}$ S/m, we ran full 3D AEM inversion independently for the subsurface resistivity distribution. We also ran a 3D inversion of the TMI data independently for the magnetization vector. Figure 5 shows the results of the independent 3D AEM inversion together with the recovered magnitude of the magnetization vector produced by an independent TMI data inversion. The magnetic anomaly shown in the left panels of this figure is too diffused to provide accurate depth information of the target, which is a typical problem for the unconstrained potential field inversion. In contrast, the conductive anomaly presented in the right panels of the same figure is more compact and has a higher depth resolution due to the multiple frequency components in the airborne EM data. The cross plot derived from the separate inversions in Figure 6, left panel, shows roughly two trends between the conductivity and magnetization. However, these trends are too cloudy to be used for the lithological identification. We also applied a joint inversion with the Gramian constraints to the same TMI and EM data to find a self-consistent anomaly associated with the kimberlite pipe in both properties and to predict their lithological relationships, if possible. The results of the joint inversion are shown in Figure 7. One can see a carrot-shaped anomaly characterized by higher magnetization and lower conductivity in this figure, which is interpreted as the kimberlite pipe. Note that the

recovered near-surface inhomogeneity outside the kimberlite pipe is conductive but nonsusceptible, which is typical for an overburden in the survey area.

Figure 6, right panel, presents a cross plot of the magnitude of the magnetization vector versus anomalous conductivity obtained from the results of the joint inversion. The two linear trends observed in the plot are associated with the kimberlite pipe (which is conductive and has an increased magnetic susceptibility) and with the near-surface inhomogeneities outside the kimberlite pipe (which is conductive but has low magnetic susceptibility), respectively. Thus, the joint inversion with Gramian constraints was able to recover multiple lithological relationships between the different physical properties of the geologic formations.

## Conclusions

Interpretation of multi-modal geophysical data represents a data fusion problem, as different geophysical fields provide information about different physical properties of the Earth. In many cases, various geophysical data are complementary and self-constraining, making it natural to consider their joint inversion based on correlations between the different physical properties of the rocks. By using Gramian constraints, we are able to invert jointly multi-modal geophysical data by enforcing the correlations between the different model parameters or their attributes. Importantly, the method assumes that a correlation between the different model parameters or their attributes exists, but the specific forms are unknown. In addition, the Gramian could be used to enhance the nonlinear relationships between the different model parameters as well. Our case studies for joint inversion of gravity gradiometry, magnetic, and electromagnetic data demonstrate how the joint inversion may enhance the produced subsurface images of the geological targets.

## Acknowledgements

The authors would like to acknowledge support from TechnoImaging and the University of Utah's Consortium for Electromagnetic Modeling and Inversion (CEMI). The authors would also like to acknowledge the Ontario Geological Survey (OGS), the Geological Survey of Canada (GSC), and Rio Tinto for providing survey data and permission to publish the results.

## References

Gallardo, L.A. and M. A. Meju [2003] Characterization of heterogeneous near-surface materials by joint 2D inversion of DC resistivity and seismic data. *Geophy. Res. Lett.*, **20** (1), 1658.

Heincke, B., M. Jegen and R. Hobbs [2006] Joint inversion of MT, gravity and seismic data applied to subbasalt imaging. *76th Annual International Meeting, SEG*, Expanded Abstracts, 784-789.

Jegen, M.D., Hobbs R.W., Tarits P. and A. Chave [2009] Joint inversion of marine magnetotelluric and gravity data incorporating seismic constraints. Preliminary results of sub-basalt imaging off the Faroe Shelf, Earth planet. *Sci. Lett.*, **282**, 47-55.

Mungall, J. E., Harvey J. D., Balch S. J., Azar B., Atkinson J. and Hamilton M.A. [2010] Eagle's nest: A magmatic Ni-sulfide deposit in the James Bay Lowlands, Ontario, Canada: Society of Economic Geologists: Special Publication, 15, 539–557.

Zhdanov, M.S. [2002] *Geophysical Inverse theory and regularization problems*. Elsevier, Amsterdam.

Zhdanov, M.S. [2009] New advances in regularized inversion of gravity and electromagnetic data. *Geophysical Prospecting*, **57**, 463-478.

Zhdanov, M.S. [2009] *Geophysical electromagnetic theory and methods*. Elsevier, Amsterdam.

Zhdanov, M.S. [2015] *Inverse theory and applications in geophysics*. Elsevier, Amsterdam.

Zhdanov, M.S., Gribenko A. and Wilson G. [2012] Generalized joint inversion of multimodal geophysical data using Gramian constraints. *Geophysical Research Letters*, 39, L09301.